

Molecular Structure of *p*-Cyclohexylaniline. Comparison of Results Obtained by X-ray Diffraction with Gas Phase Laser Experiments and ab Initio Calculations

Christoph Riehn,^{*,†} Alexander Degen,[‡] Andreas Weichert,[†] Michael Bolte,[‡] Ernst Egert,[‡] Bernhard Brutschy,[†] P. Tarakeshwar,[§] and K. S. Kim[§]

Institut für Physikalische und Theoretische Chemie, Johann Wolfgang Goethe-Universität Frankfurt/M., Marie-Curie-Strasse 11, D-60439 Frankfurt/M., Germany; Institut für Organische Chemie, Johann Wolfgang Goethe-Universität Frankfurt/M., Marie-Curie-Strasse 11, D-60439 Frankfurt/M., Germany; and Department of Chemistry, National Creative Research Initiative Center for Superfunctional Materials, Pohang University of Science and Technology, San 31, Hyojadong, Pohang 790-784, Korea

Received: March 7, 2000; In Final Form: September 26, 2000

The results of a combined experimental and theoretical investigation of the molecular structure of *p*-cyclohexylaniline (pCHA) in the electronic ground and the first electronically excited state are reported. The experimental investigations are performed for the crystalline phase by X-ray diffraction for the first time and related to former gas phase results obtained by time-resolved rotational laser spectroscopy. The theoretical results, from new ab initio calculations at the MP2/6-31+G(d) and CIS/6-31+G(d) level of theory for the electronic ground and excited state, respectively, give an adequate description of the rotational constants as obtained by the gas phase experiments. Thus, a detailed comparison of the ab initio structure for the ground state with the X-ray structure is performed in order to ascertain differences in the molecular geometry between the gas and crystalline phase. In particular, the size of the aromatic and cyclohexyl ring, their mutual orientation, and the conformation of the NH₂ group are affected. The latter can be ascribed to intermolecular hydrogen bonding forming chainlike structures in the crystalline phase. Moreover, the results of the ab initio calculations allow for a discussion of the structural changes of pCHA upon photoexcitation in the gas phase.

I. Introduction

Recently, the structural investigation of aniline and substituted anilines has attracted considerable attention due to their importance as model systems for intramolecular charge transfer after photoexcitation. In particular, the ground state structures of *N*-methylated *p*-cyanoanilines (aminobenzonitriles) have been obtained from X-ray diffraction¹ and the relevance of the obtained geometries has been discussed as starting point for intramolecular charge transfer in the first electronically excited state after vertical photoexcitation.¹ For aniline^{2–6} and a variety of aniline derivatives,^{7–11} the influence of the electronic interaction between the amino group and the aromatic π -electron system on the molecular structure has been investigated for both the electronic ground (S_0) and excited state (S_1) in the gas phase. For instance, the electronic spectroscopy and the conformations of *p*-alkylanilines (with *n*-alkyl chains) have been studied by laser-induced fluorescence (LIF) spectroscopy.⁸ *p*-Alkoxyanilines with different alkyl chain lengths and *p*-hydroxyaniline have been used to study by LIF the onset of internal vibrational relaxation (IVR).^{9,10} The molecular structure and the vibrations in the excited state of *p*-fluoroaniline have been investigated by laser-induced resonant two-photon ionization (R2PI) in combination with ab initio calculations.¹¹ In order to investigate intermolecular interactions under well-defined conditions, the aniline dimer has been interrogated by gas phase IR/R2PI laser

spectroscopy and evidence for an antiparallel stacked structure with mutual NH₂... π bonds has been reported.¹² These results are contrasted by X-ray investigations in the solid state of aniline,¹³ aminobenzonitriles,¹ and nitroaniline.¹⁴

In this report, we present results of a combined study of theory and experiment to elucidate the ground state as well as the first excited state molecular structure of *p*-cyclohexylaniline (pCHA). The phenylcyclohexane skeleton is a common mesogenic core of compounds, which exhibit liquid crystal behavior.¹⁵ Thus, a detailed knowledge of the structure might be helpful for understanding the molecular basis of this phenomenon. We applied X-ray diffraction and laser rotational coherence spectroscopy (RCS)¹⁶ in order to obtain structural information. Furthermore, ab initio calculations have been performed to describe the gas phase structure and to investigate the molecular coordinates. In a previous publication, we already presented the high-resolution laser RCS results and discussed partially the changes in structure upon electronic excitation of pCHA.^{17,18} Here we focus on the ground state structure and present the first X-ray diffraction results of pCHA in the crystalline phase and new results of ab initio calculations including electron correlation. In particular, we will discuss intermolecular hydrogen bonding observed in the crystal and its influence upon the molecular structure. These results demonstrate that a careful inspection of X-ray structures has to precede their application for the analysis of experiments in the gas phase.

II. Experimental Section

A. X-ray Diffraction. The title compound was purchased from Lancaster (No. 3184, purity 97%). Single crystals were grown by slow evaporation from *n*-hexane.

* Corresponding author. E mail: riehn@chemie.uni-frankfurt.de.

[†] Institut für Physikalische und Theoretische Chemie, Universität Frankfurt/M.

[‡] Institut für Organische Chemie, Universität Frankfurt/M.

[§] Pohang University of Science and Technology, Department of Chemistry.

TABLE 1: Crystal Data, Data Collection, and Refinement Parameters for pCHA

empirical formula	C ₁₂ H ₁₇ N
formula weight (g mol ⁻¹)	175.27
temperature (K)	173(2)
wavelength (Å)	0.71073
crystal system	Monoclinic
space group	<i>P</i> 2 ₁ / <i>c</i>
unit cell dimensions	<i>a</i> = 14.552(1) Å, <i>b</i> = 5.591(1) Å, <i>c</i> = 13.302(1) Å β = 107.88(1)°
volume (Å ³)	1030.0(2)
<i>Z</i>	4
calculated density (Mg/m ³)	1.130
absorption coefficient (mm ⁻¹)	0.065
<i>F</i> (000)	384
crystal size (mm ³) and habit	0.42 × 0.36 × 0.22, colorless block
θ range for data collection (deg)	1.47 to 26.37
index ranges	-18 ≤ <i>h</i> ≤ 18, -6 ≤ <i>k</i> ≤ 6, -16 ≤ <i>l</i> ≤ 16
reflections collected	17204
independent reflections	2098 [<i>R</i> (int) = 0.0837]
completeness to $\theta = 26.37^\circ$	100%
absorption correction	empirical ¹⁹
refinement method	full-matrix least-squares on <i>F</i> ²
data/restraints/parameters	2098/0/127
goodness-of-fit on <i>F</i> ²	1.020
final <i>R</i> indices [<i>I</i> > 2σ(<i>I</i>)]	<i>R</i> ₁ = 0.0729, <i>wR</i> ₂ = 0.1510
<i>R</i> indices (all data)	<i>R</i> ₁ = 0.1664, <i>wR</i> ₂ = 0.1921
extinction coefficient	0.009(4)
$\Delta\rho_{\max}$, $\Delta\rho_{\min}$ (e Å ⁻³)	0.202 and -0.187

The X-ray intensities for the structure determination were collected on a Siemens (now Bruker AXS) SMART CCD diffractometer at *T* = 173 K using graphite monochromated Mo *K*α radiation. After data reduction, an empirical absorption correction was applied.¹⁹

The structure was solved by direct methods and subsequent Fourier syntheses and was refined by full-matrix least-squares techniques with anisotropic displacement parameters using the programs SHELXS-97²⁰ and SHELXL-97.²¹ The positions of the H atoms were located by difference Fourier synthesis. The amino H atoms were refined freely, all others with fixed individual displacement parameters [*U*(H) = 1.2*U*_{eq}(C)] using a riding model with C–H(aromatic) = 0.95, C–H(secondary) = 0.99 or C–H(tertiary) = 1.0 Å. The molecular graphics were obtained with XP in SHELXTL-Plus.²² Further details are given in Table 1.

B. Rotational Coherence Laser Spectroscopy. For a more detailed description of the experimental setup of the picosecond laser system and the molecular beam apparatus we refer to previous publications.^{17,18} Here, we will give only the principal concept of this high-resolution laser technique. Rotational coherence spectroscopy (RCS) is a time-resolved rotational laser spectroscopy, which is preferentially applied to large molecules and molecular clusters in the gas phase under molecular beam conditions.^{23,24} For the experiment a supersonic gas expansion is employed, resulting in a rotational temperature of the molecules of ≈10 K and a vibrational temperature of ≈100 K, i.e., comparable to that in the X-ray experiment. This laser technique is complementary to frequency-resolved spectroscopic techniques such as high-resolution laser fluorescence or absorption spectroscopy and microwave spectroscopy. The main experimental results derived by it are the rotational constants for the electronic ground and excited state of the molecular system under study. The precision of the rotational constants lies in the sub-MHz range, giving a relative accuracy of ≈10⁻⁴.

The underlying physical process can be understood classically in terms of an ultrafast laser experiment, in which the rotational

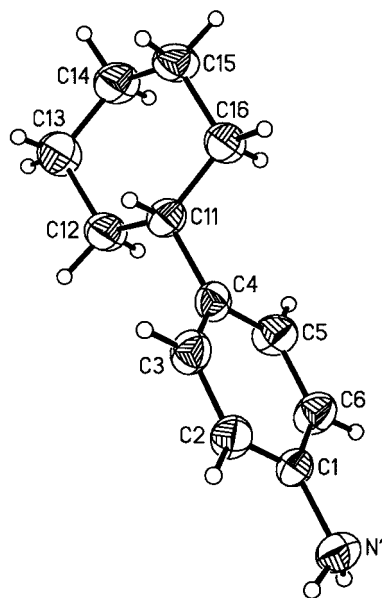


Figure 1. Structure of *p*-cyclohexylaniline from X-ray diffraction. Displacement ellipsoids are shown at the 50% probability level.

periods of molecules are measured in “real-time”. This is accomplished by the use of a linear polarized picosecond pump laser pulse, in order to selectively excite molecules at *t* = 0, which are aligned with their transition dipole moments parallel to the electric field of the laser, followed by a time-resolved polarization-sensitive detection. Due to the free rotational motion of the molecules, the initial alignment decays within a few picoseconds, but a recovery of this alignment is obtained after a characteristic rotational period. In the experimental setup employed, a picosecond probe laser pulse with the same wavelength, intensity, and polarization as the pump pulse was used for detection, and the time- and wavelength-integrated fluorescence signal as a function of the time delay between both pulses was recorded (time-resolved fluorescence depletion, TRFD).^{25,26} The RCS spectrum exhibits several recurrence transients, which can be related to algebraic combinations of the rotational constants (in the time domain) of the molecule.¹⁶

From a quantum mechanical point of view, RCS has to be considered as a thermally averaged rotational quantum-beat spectroscopy. Comprehensive accounts on the theoretical basics and the simulation and analysis of the resulting spectra are given in the literature.²⁷

III. Results

A. X-ray Data. As a result of the X-ray diffraction analysis, the atomic coordinates and the corresponding anisotropic displacement parameters of pCHA are given in the Supporting Information in Tables 1S and 2S, respectively. The obtained molecular structure of pCHA in the crystalline phase at 173 K is depicted in Figure 1 together with the numbering of the atoms. In Table 2 selected structural parameters are listed for comparison with the theoretical results describing the gas phase structure. In Table 3 parameters of the intermolecular hydrogen bond are given together with the corresponding data of aniline.¹³

B. RCS Data. The results of the RCS study of pCHA are summarized in Table 4, together with the corresponding ab initio and X-ray data. The rotational constants of the RCS experiment are obtained by an extensive numerical fitting procedure based on the simulation of the RCS spectra. Details of the procedure, especially the error analysis, and a discussion of the results are given in ref 18.

TABLE 2: Selected Structural Parameters of the X-ray Diffraction Experiment and the ab Initio Geometry Optimization (MP2/6-31+G(d) and CIS/6-31+G(d) Level) for pCHA

		experimental results (S ₀ , X-ray diffraction)	ab initio calculation (S ₀) MP2/6-31+G(d)	ab initio calculation (S ₂) ^a CIS/6-31+G(d)	
Bond Lengths/Å					
NH ₂ group	N–H(1A)	0.86(3)	1.016	0.995	
	N–H(1B)	0.91(4)	1.016	0.995	
aromatic ring	N–C(1)	1.414(4)	1.409	1.340	
	C(1)–C(2)	1.368(4)	1.402	1.425	
	C(1)–C(6)	1.390(4)	1.404	1.421	
	C(2)–C(3)	1.383(4)	1.397	1.403	
	C(3)–C(4)	1.380(4)	1.402	1.416	
	C(4)–C(5)	1.380(4)	1.405	1.416	
	C(5)–C(6)	1.383(4)	1.395	1.405	
	long axis short axis	C(1)–C(4)	2.814	2.844	2.810
		C(2)–C(6)	2.368	2.410	2.481
		C(4)–C(11)	1.513(4)	1.508	1.510
phenylcyclohexyl cyclohexyl ring	C–C ^b	1.517	1.531	1.535	
	long axis	C(11)–C(14)	2.958	2.962	2.972
	short axis	C(12)–C(16)	2.492	2.519	2.527
Bond Angles/deg					
NH ₂ group	H(1A)–N–H(1B)	110(3)	110.1	117.7	
	H(1A)–N–C(1)	112(2)	113.7	121.1	
aromatic ring	H(1B)–N–C(1)	113(2)	113.7	121.2	
	C(2)–C(1)–N	122.1(3)	120.8	119.1	
	C(6)–C(1)–N	119.6(3)	120.6	119.5	
	C(2)–C(1)–C(6)	118.3(3)	118.4	121.3	
	C(1)–C(2)–C(3)	120.9(3)	120.5	118.6	
	C(4)–C(3)–C(2)	121.9(3)	121.7	120.7	
	C(3)–C(4)–C(5)	116.8(3)	117.4	119.9	
	C(4)–C(5)–C(6)	122.1(3)	121.4	120.5	
	C(5)–C(6)–C(1)	120.1(3)	120.7	118.9	
	NH ₂ wagging	NH ₂ -phenyl plane	47.8	45.5	0.0
cyclohexylphenyl bend (ip) ^c	C(3)–C(4)–C(11)	120.4(3)	121.0	119.1	
cyclohexylphenyl bend (oop) ^d	C(4)–C(11)–C(12)	111.5(2)	112.1	112.6	
Dihedral Angles/deg					
NH ₂ twisting	H(1A)–N–C(1)–C(2)	16(3)	28.5	0.0	
	H(1B)–N–C(1)–C(2)	141(2)	155.5	180.0	
	H(1A)–N–C(1)–C(6)	–166(2)	–156.5	180.0	
	H(1B)–N–C(1)–C(6)	–40(2)	–29.5	0.0	
	N–C(1)–C(2)–C(3)	179.1(3)	176.4	180.0	
	N–C(1)–C(6)–C(5)	179.9(3)	–176.5	180.0	
cyclohexylphenyl twisting	C(5)–C(4)–C(11)–C(16)	–52.9	–62.2	–62.5	

^a S₂ corresponds to the experimentally observed excited state (see text). ^b Average value. ^c ip: in the phenyl plane. ^d oop: out of the phenyl plane.

TABLE 3: Intermolecular Hydrogen Bond Parameters in the Crystalline Phase of *p*-Cyclohexylaniline (pCHA) and Aniline Determined by X-ray Diffraction (Å and deg)

D–H···A	<i>d</i> (D–H)	<i>d</i> (H···A)	<i>d</i> (D···A)	∠(DHA)
pCHA ^a				
N1–H1A···N1 (i) ^c	0.86(3)	2.40(4)	3.247(3)	166(3)
aniline ^b				
N1–H10···N2 (ii) ^c	1.07(5)	2.16(5)	3.180(6)	159(4)
N2–H200···N1 (iii) ^c	0.99(4)	2.43(3)	3.373(5)	158(3)

^a This work. ^b From ref 13. ^c Symmetry transformations used to generate equivalent atoms: (i): $-x + 1, y - 0.5, -z + 1.5$; (ii): $x, -y + 0.5, z + 0.5$; (iii): $x, y, z - 1$.

C. Computational Results. In order to gain insight into the molecular geometry we performed ab initio calculations for both the ground and excited states of pCHA using the 6-31+G(d) basis set containing 268 basis functions. In the case of the ground state (S₀), calculations at both the Hartree–Fock (HF) and the second-order Møller–Plesset perturbation (MP2) levels of theory were performed. The excited state calculations were carried out using the configuration interaction singles (CIS) method. Here we applied also the aug-cc-pVDZ basis set containing 452 basis functions. The results were similar to the CIS/6-31+G(d) level, so that only these will be reported and

discussed. Complete geometry optimizations were carried out at all levels applying standard convergence criteria and checked for true minima. All frequencies in the harmonic approximation were real. While pCHA has a C₁ symmetry in the ground state, in the excited state the molecule has a C_s symmetry with the aromatic plane as a mirror plane. Since calculations reveal that the electronic properties of the C₁ and C_s symmetric species are exactly the same in the excited state, the results obtained on the C₁ symmetric species are only reported in this study. Selected structural parameters are given in Table 2, and the resulting rotational constants are listed in Table 4. All calculations reported in this study were carried out using the Gaussian 94 suite of programs.²⁸

Before we compare the results obtained from the ab initio calculations to the X-ray data, it is useful to examine the role of basis set size and the level of correlation in describing the experimental geometries and rotational constants of similar molecules. In a study by Lampert et al., the geometries of a number of aromatic molecules (benzene, phenol, benzaldehyde, salicylaldehyde) were evaluated at various levels of theory using different basis sets.²⁹ They found that the best correspondence between the experimental and theoretical calculations is obtained at the MP2 and the density functional (B3LYP) levels of theory

TABLE 4: Rotational Constants of pCHA (in MHz) As Obtained by RCS, ab Initio Calculations and X-ray Diffraction Analysis

	<i>p</i> -cyclohexylaniline			aniline		
	RCS ^a (gas phase)	ab initio ^b	X-ray diffraction (solid state) ^b	high-resolution (gas phase) ^c	ab initio	X-ray diffraction (solid state) ^d
	Ground State (S ₀)					
<i>A</i>	2406.4 ± 0.6	2408.7	2538.2 ± 13.5	5618.1 ± 0.2	5596.8 ^b	5893.4 (5866.1) ± 58
<i>B</i>	358.3 ± 0.3	358.5	364.7 ± 0.6	2594.2 ± 0.2	2581.0 ^b	2616.0 (2638.7) ± 17
<i>C</i>	356.5 ± 0.3	357.1	357.7 ± 0.6	1777.2 ± 0.2	1769.8 ^b	1814.6 (1823.3) ± 10
<i>B + C</i>	714.8 ± 0.4	715.6	722.4 ± 1.2			
	Carbon Skeleton (S ₀) ^e					
<i>A</i>		3268.9	3370.6			
<i>B</i>		401.5	407.1			
<i>C</i>		400.9	400.2			
	Excited State					
<i>A</i>	2346.3 ± 1.3	2377.3		5286.9 ± 0.2	5466.8 ^f	
<i>B</i>	362.9 ± 1.8	360.7		2633.8 ± 0.2	2712.9 ^f	
<i>C</i>	356.4 ± 1.8	358.7		1759.4 ± 0.2	1813.2 ^f	
<i>B + C</i>	719.3 ± 2.1	719.4				

^a From ref 18. ^b This work. Calculations were performed for ground state (S₀) at MP2/6-31+G(d) level, excited state (S₂) at CIS/6-31+G(d) level. ^c From ref 2. ^d From ref 13. ^e Since the C–H bonds have not been well resolved in the X-ray analysis of this work, the rotational constants of the carbon skeleton including the amino group were calculated from the X-ray and ab initio data. ^f From ref 5.

(the mean absolute deviations of the rotational constants are less than 0.2%). On the other hand, the rotational constants calculated at the HF level are consistently higher than the experimental numbers. Compared to the experimental bond lengths, the aromatic C–C bond lengths are slightly longer, and the C–O, C=O bond lengths are slightly shorter at the MP2 level. Hence, the rotational constants are more reflective of the overall structure than specific geometrical parameters.

Since pCHA contains an amino group, we highlight the effect of an increase in the basis set size and the level of correlation on the geometries using the calculations carried out by us on aniline.³⁰ The most significant structural changes accompanying basis set augmentation from 6-31+G(d) to aug-cc-pVDZ at the MP2 level are an elongation of the N–C and C–C bonds by ca. 0.01 Å and shortening of the N–H and C–H bonds by ca. 0.005 Å. As in the case of benzene, phenol, and benzaldehyde, the calculated distances are comparatively higher than the corresponding experimental distances obtained from the rotational spectra of aniline.⁴

IV. Discussion and Structural Differences between Gas Phase and Solid State

In the following we will use the data on the bond lengths and angles of the ab initio calculation to represent the structure of pCHA in the gas phase (Table 2). We concentrate here on the ground state structure, which will be compared for different structural regions of the molecule with the results of the X-ray diffraction analysis. The intermolecular interactions in the crystalline phase and its consequences for the molecular structure will be discussed based on the crystal packing data.

Since the experimental structural data of pCHA in the gas phase are rotational constants it is pertinent to estimate the sensitivity of these constants to selective structural parameters. In an earlier publication we have discussed this relation in detail on the basis of ab initio calculations at the HF/6-31G(d) level.¹⁸ Simple one-dimensional model calculations were performed by modification of molecular coordinates from their ab initio optimized values and normalization of the resulting rotational constants with respect to the experimentally determined values. By this method the two inter-ring bending modes (in the phenyl plane, out of the phenyl plane) and the inter-ring torsion were explored. We obtained a variation of the rotational constants

of 0.5% upon change of the bending angles ($\angle C(3)–C(4)–C(11)$, $\angle C(4)–C(11)–C(12)$) by 3° and also by change of 5° of the torsion dihedral angle ($\angle C(5)–C(4)–C(11)–C(16)$). For the torsional angle it is obvious that the *A* constant along the prolate top axis (long axis of the molecule) is less sensitive than the *B* and *C* constant perpendicular to it. A more detailed description can be found in ref 18. If one considers that the relative experimental errors of the rotational constants are an order of magnitude smaller than the obtained variations, a comparison of gas phase, i.e., ab initio structure and X-ray structure, is justified for the inter-ring coordinates.

We have also analyzed the dependence of the rotational constants on direct variation of certain bond lengths and found that small increases (~0.01 Å) in the lengths of the C(1)–C(2)/C(1)–C(6) bonds leads to a decrease in the value of *A* by about 14 MHz (0.6%). The effect of this increase on the sum of *B* and *C* is considerably smaller (~1 MHz, 0.1%). Except for the C(4)–C(11) bond (sum of *B* and *C* decreases by about 2 MHz, 0.3%, for an increase in the bond length by 0.01 Å), the increase in the lengths of all the other bonds has a small effect (decreases by about 1 MHz, 0.1%, for an increase in the bond length by 0.01 Å) on the sum of *B* and *C*. Obviously *A* is invariant to increases in the C(4)–C(11) bond lengths. Increases in the lengths (~0.01 Å) of the other bonds, C–N, C(2)–C(3), and C(3)–C(4), leads to a small decrease (~1 MHz, 0.04%) of *A*. In the course of our discussion on the geometries of the excited states, we show how these geometrical changes can help explain the observed changes in the rotational constants of the excited state of pCHA.

Obviously, the conformation of the amino group has a much smaller influence on the rotational constants. An estimation amounted to about a 2 order of magnitude smaller change in the rotational constants. But here a note of caution is appropriate. In the applied method no relaxation or optimization of other coordinates at the new geometry was performed. Since the interaction between the aromatic and the cyclohexyl ring is negligible, this procedure is justified for the inter-ring coordinates. However, for the amino group it was pointed out before for the case of aniline² that an optimization of the geometry is indispensable in order to account correctly for the electronic interaction. For pCHA these calculations have not been performed and thus a definitive assessment cannot be given yet.

Another point noteworthy is that small variations in rotational constants can also be achieved upon changing slightly several coordinates at the same time. For instance, the conformation of the amino group of *p*-aminobenzonitrile in the electronically excited state has been analyzed and two contrary values for the wagging angle based on the same rotational constants have been published (34° in ref 31, 0° in ref 32). Thus, an unambiguous conformational analysis of the amino group based on the rotational constants alone is not feasible and ancillary spectroscopic information, e.g., from vibronic spectra, has to be taken into account.

However, since the results of our calculation are in line with corresponding data of a series of aniline derivatives,^{1–7} we think that the following detailed discussion is well-founded. Moreover, it is useful for a deeper understanding of the structural change of this class of molecules going from the gas to the crystalline phase.

A. Overall Structure. The general molecular structure of pCHA is similar for both the gas and the crystalline phase. The cyclohexyl ring is connected to the phenyl ring by an equatorial bond. Both rings are oriented nearly perpendicular with respect to their “short axes”. The “long axes” of both rings are nearly in the same plane and inclined to each other by an angle of 24° . If, in a simplified picture, the “inter-ring” torsion and asymmetric distortions are ignored, the phenyl plane would be a mirror plane (point group C_s). Upon inclusion of a nonplanar amino group, two enantiomeric structures could be constructed, but they are interconverted readily in the gas phase by tunneling in the symmetric double well potential. In general, the bond angles for the crystalline and gas phase data agree fairly well (within 1%), except for the angles related to the amino group and the inter-ring angles. The dihedral angles show slightly larger differences.

B. Conformation of the NH₂ Substituent. The NH₂ group has a pyramidal character in both phases as demonstrated by the wagging angle of 47.8° and 45.5° for the X-ray structure and the ab initio calculation, respectively.³³ Furthermore, the sum of the angles around the nitrogen atom is 335° for the X-ray structure (337.5° for the ab initio data) which is closer to a sp^3 (328.4°) than a sp^2 (360°) character. The twist angle of the NH₂ group in the gas phase is negligible whereas in the crystal there is a considerable amount of twisting (around 11° – 14° from the symmetric structure) to accommodate to the intermolecular hydrogen bonding (see below). This points toward a slightly stronger interaction of the amino group with the aromatic ring for the gas phase structure as compared to the X-ray structure. For both structures the N atom lies nearly in the phenyl plane, i.e., the distance between N(1) and the least-squares plane given by the carbon atoms C(1) through C(6) is small; 0.004 \AA in the X-ray, 0.013 \AA in the ab initio structure. This is in contrast to aniline, where a displacement of the N atom out of the phenyl plane to the opposite side as the H atoms by 0.12 \AA has been obtained from its X-ray structure.¹³

C. Aromatic Ring. The aromatic ring is slightly distorted from a regular hexagon. For both sets of data the endocyclic angles $\angle C(2)-C(1)-C(6)$ and $\angle C(3)-C(4)-C(5)$ at the substitution positions are smaller than 120° , whereas the other angles are larger. In the ab initio structure the bonds C(2)–C(3) and C(5)–C(6), parallel to the long axis, are smaller than the remaining C–C distances in the ring. This quinoidal character is strongly increased upon electronic excitation (see ref 15 and discussion below). In the X-ray structure no systematic variation of the aromatic C–C bond distances is observed. However, the C–C bonds of the substituted atom C(1)

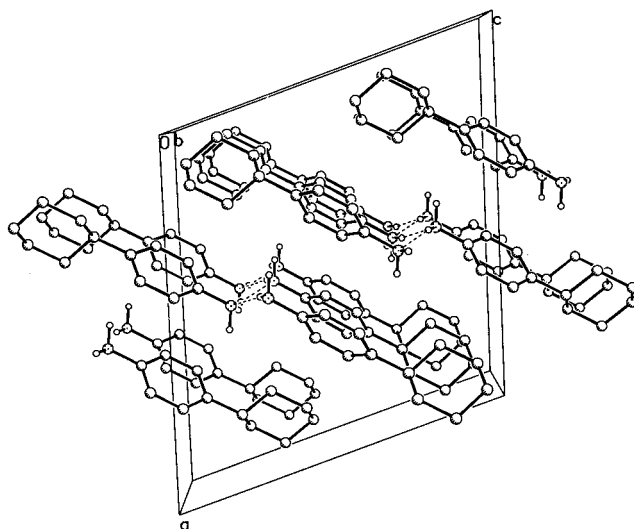


Figure 2. Crystal packing of *p*-cyclohexylaniline obtained by X-ray diffraction (view along the *b*-axis).

represent the longest (1.390 \AA) and the shortest bond (1.368 \AA) in the aromatic ring, presumably due to the modified conformation of the amino group and its involvement in an intermolecular hydrogen-bonded chain. Interestingly, a similar behavior was obtained from the X-ray structure of aniline, where the aromatic C–C bond *cis* to the N–H bond, which is involved in the hydrogen bond, also exhibits the largest aromatic bond length. In the case of pCHA, a comparison of the long and short axes of the aromatic ring shows that the ring in the crystal is significantly smaller than in the gas phase (by 1–2%). Note also that there is a systematic underestimation in the calculated bond lengths by the employed ab initio methods.²⁹

D. Cyclohexyl Ring. The cyclohexyl ring resides in its low-energy chair conformation. The overall ring size in the crystalline phase, given by the corresponding long and short axis, is smaller by approximately 1% compared to the gas-phase value. However, the C–C bond distances in the ring show larger “fluctuations” for the crystalline phase than for the gas phase. A more pronounced difference between both structures can be found in the detailed inspection of the relative orientation of the cyclohexyl and phenyl ring. In the X-ray structure a twisting along the C(4)–C(11) bond by 9° is observed (Table 2, $\angle C(5)-C(4)-C(11)-C(16)$). However, the inter-ring bending coordinates in and out of the phenyl plane show only very small differences (approximately 0.6°) between both phases. For both structures the influence of the cyclohexyl ring on the aromatic system seems to be negligible, which is comparable to data for *p*-methylaniline.⁷

E. Crystal Packing and Intermolecular Interactions. The crystal structure of pCHA is stabilized by an intermolecular hydrogen bond (Figure 2, Table 3) with a $NH\cdots N$ hydrogen bond length of $2.40(4) \text{ \AA}$ and a $N\cdots N$ distance of $3.247(3) \text{ \AA}$. It is remarkable that it is the H atom H(1A) which nearly lies in the plane of the aromatic ring ($\angle H(1A)-N(1)-C(1)-C(2) = 16^\circ$) that is involved in the hydrogen bond and not the other amino hydrogen atom H(1B), which is twisted by approximately 40° (see Table 2) out of the plane of the phenyl ring. The two N–H bond lengths have nearly the same value with $0.86(3) \text{ \AA}$ (N–H(1A)) and $0.91(4) \text{ \AA}$ (N–H(1B)). However, only one hydrogen atom in each amino group is involved in the hydrogen bonding. Thus, each amino group acts both as a donor and an acceptor in a hydrogen bonded zigzag chain connecting two face-to-face oriented stacks of pCHA molecules (Figure 3).

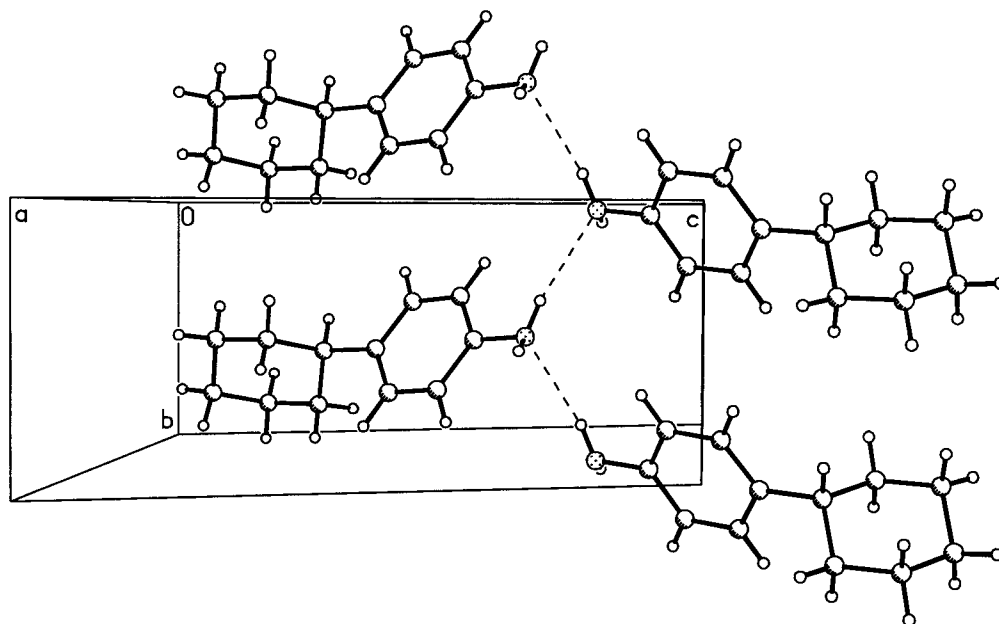


Figure 3. Intermolecular hydrogen bonds in the crystalline phase of *p*-cyclohexylaniline obtained by X-ray diffraction.

For comparison, the X-ray analysis of aniline at 252 K revealed a similar intermolecular arrangement.¹³ The crystal structure of aniline contains two nearly identical molecules (rmsd: 0.012 Å fitting all non-H atoms) per asymmetric unit which are hydrogen bonded and form infinite chains. This pattern is similar to the one found in pCHA, except that the two N···N distances are significantly different (3.180(6) and 3.373(5) Å; see Table 3 for further details). Interestingly, this intermolecular structure in the crystal is clearly distinct from the results of an antiparallel stacked aniline dimer in the gas phase,¹² demonstrating that the solid state behavior of organic crystals will only be reached in larger homogeneous aggregates.

A possible explanation for the differences between the pCHA and aniline structure in the crystalline phase can be obtained from consideration of the voluminous cyclohexyl substituent. This group, oriented nearly perpendicular to the aromatic ring, acts as a spacer between pCHA molecules within a stack.

F. Comparison of Rotational Constants. Since the rotational constants of pCHA are the direct experimental results of our RCS laser study in the gas-phase we calculated also the rotational constants from the X-ray and the ab initio data for comparison (Table 4). The experimental uncertainties of the X-ray data have also been propagated appropriately by means of a Monte Carlo method to achieve the corresponding error margins of the rotational constants. In Table 4 we listed likewise artificial rotational constants for the carbon skeleton of pCHA, i.e., without carbon bound hydrogen atoms, because the latter have not been well resolved in the X-ray experiment. From the data in Table 4 it is noticeable that the rotational constants *A* and *B* of the molecule in the crystalline phase are significantly larger than those of the isolated molecule. This can be rationalized by a compression of the molecular frame in the crystalline phase. From the bond lengths of Table 2 one can deduce that the compression along the long axis of the molecule (*a* axis in the molecular frame) is much less than the compression perpendicular to this axis, leading to a strong increase in the *A* rotational constant whereas *B* and *C* are only moderately increased. Furthermore it is obvious from Table 4 that the results of the ab initio calculation serve as an excellent representation of the gas phase structure, which is the basis for the detailed structural discussion presented above.

The gas phase measurements exhibit smaller uncertainties than the crystalline phase X-ray results. However, note that rotational constants given by the moments of inertia of the principal axes by definition represent an integration over mass-weighted coordinates of the molecular system. Moreover, with three rotational constants, no unambiguous recovery of all molecular coordinates of pCHA, composed of 30 atoms, is possible. Thus, although the uncertainties for the rotational constants obtained from the X-ray analysis are larger, the information content of the X-ray data is obviously higher since atomic coordinates are unambiguously obtained.

For the molecule aniline, which represents the UV chromophore unit of pCHA, corresponding sets of data (gas phase, ab initio, crystalline phase) have been collected from the literature and are listed in Table 4. The increase of the rotational constants in going from the gas phase to the crystalline phase is very similar. The effect on the *A* rotational constant is less pronounced due to the smaller size of the one-ring system aniline. Note that the rotational constants of the two structures for aniline of ref 13 are accompanied by uncertainties (2 σ confidence interval) which do not allow for an unambiguous assignment. As discussed above, the intermolecular interactions in the crystalline phase are dominated by hydrogen bonding mediated by the amino groups and thus are very similar to pCHA.

V. Structural Changes upon Photoexcitation of pCHA in the Gas Phase

The changes of the molecular structure upon electronic excitation of pCHA to the S_1 state have been discussed in previous publications.^{18,34} Here, we review the main features, substantiated by results of new high-level ab initio calculations. Since these new calculations have been carried out using basis sets containing diffuse functions, the description of the excited states should be more reliable. To the best of our knowledge, there have been few studies detailing the performance of different theoretical methods in characterizing the geometries of the excited state of large molecules. The focus of most calculations on the excited state have been in evaluating the vertical excitation energies, the oscillator strengths, etc.³⁵

However, recent studies of the excited states of benzene, styrene, and aniline using the CIS method seem to indicate that the method can be employed to obtain reasonably accurate geometries.^{4,36,37}

Upon photoexcitation, the experimental rotational constants (Table 4) exhibit a decrease of *A* by 2.6%, and a small increase of *B*, whereas *C* nearly stays constant (set II of ref 18).³⁸ To account for the structural changes we will use the results of the new ab initio calculation in the following, justified by the good agreement of experimental and theoretical rotational constants for both electronic states.

But before doing that, it is imperative for us to indicate that the calculated excited state structure corresponds to the structure being observed in the experiments. In our earlier calculations using the 6-31(d) basis set, the first three singlet excited states of pCHA evaluated by the CIS method had nonzero oscillator strengths. Hence, the calculated S_1 state was attributed to the experimentally observed excited state. The use of the 6-31+G(d) basis set, however, leads to a lot of changes in the structures of the excited states of pCHA. Interestingly, there is little difference in the structures of the excited states of pCHA, when the much larger aug-cc-pVDZ basis set is used. This seems to give an impression that the 6-31+G(d) basis set is quite adequate in representing the excited state. However, we believe that more sophisticated theoretical methods like CASPT2, CCSD, and MRD-CI have to be employed to observe the effect of the change in the basis set from the 6-31+G(d) to the much larger aug-cc-pVDZ. Initially we carried out an optimization of structure of pCHA in the first excited state (S_1). A large increase in the dipole moment with respect to the ground state and a vertical excitation energy of 4.86 eV was found, but the oscillator strength was zero. The second excited state (S_2), however, had a nonzero oscillator strength ($f = 0.10$). Hence we thought that the experimentally observed excited state might correspond to the second excited state. We therefore carried out an optimization of the structure of pCHA in this state. There are significant differences in the structures of the S_1 and S_2 optimized geometries, and hence the calculated rotational constants are also different. A vertical excitation energy of 5.17 eV was obtained for the S_2 excited state optimized structure, which indicated that the excitation energies of both the S_1 and S_2 excited states are very close to each other. Given the nonzero oscillator strengths of the S_2 excited state of pCHA, we believe that the S_2 excited state optimized structure corresponds to the experimentally observed excited state (4.13 eV).^{18,34} Furthermore, this is corroborated by the alignment of the transition dipole moment, which is in-plane short-axis polarized with respect to the aromatic ring for the S_2 excited state in agreement with the experimental findings.

Some of the salient geometrical features of the S_2 excited state optimized structure are listed in Table 2. It can be seen from the geometry listed in Table 2 that the excited state structure of pCHA possesses a C_s symmetry. Furthermore, the data in Table 2 indicate that in the excited state there is a significant shortening of the C–N bond accompanied by a planarization of the NH_2 group (wagging angle $\approx 0^\circ$), which allows for a stronger interaction of the NH_2 group with the aromatic ring. The bond length between the two ring systems is also slightly decreased, but there is little effect on the inter-ring twisting or bending coordinates. As expected for a local excitation in the aromatic chromophore, the cyclohexyl ring does not change in size, whereas the aromatic ring increases considerably. Particularly, the short axis (distance C(2)–C(6) in Table 2) increases by 2.0%, whereas the ring contracts slightly

along the long axis (-0.9%), resulting in a decrease of the *A* rotational constant and a small increase in *B* and *C*. In the beginning of this section, we had discussed the effect of changes in various bond lengths on the rotational constants. In particular, we had pointed out that the increase of the C(1)–C(2)/C(1)–C(6) bond lengths leads to a decrease in the rotational constant *A*. It is interesting to note that in the excited state both these bonds exhibit significant lengthening. These structural changes agree with an augmented contribution of the quinoidal resonance structure of pCHA in the electronically excited state. From the increase of the $\angle HNH$ and $\angle HNC(1)$ angle by 7° – 8° it can also be concluded that the interaction of the lone-pair electrons in the amino substituent and the π -electrons is increased in the excited state. This photophysical behavior agrees well with corresponding experimental and theoretical results on aniline^{2–6} and *p*-methylaniline.⁷

VI. Conclusions

In this study, the X-ray structure of *p*-cyclohexylaniline is reported for the first time. The structural data are compared with former high-resolution gas phase experiments, which were analyzed by a new ab initio calculation.¹⁸

Although the general features of the structure in the gas and crystal phase compare well, a detailed examination reveals systematic differences. In the crystalline phase the molecular carbon skeleton is slightly compressed, and an intermolecular hydrogen bond causes approximately a 10° torsion of the amino group. This torsion might affect slightly the structure of the aromatic ring, most probably by modification of the interaction of the free electron pair of the amino group and the aromatic π -electron system. Moreover, presumably as a result of π -stacking in the crystalline phase a tilt by 9° between the cyclohexyl and the aromatic ring compared to the gas phase structure is detected. The general results agree well with studies on similar compounds in the crystalline and the gas phase, e.g., aniline,^{2–6} *p*-methylaniline,⁷ and aminobenzonitriles.¹

Acknowledgment. We gratefully acknowledge the Hermann-Willkomm-, Adolf-Messer-, and Bodo-Sponholz-Stiftung. P.T. and K.S.K. are thankful for support by MOST/STEPI under the creative research initiatives program.

Supporting Information Available: Detailed information on the X-ray diffraction experiment concerning the atomic coordinates and the anisotropic displacement parameters for pCHA is reported in Table 1S and Table 2S, respectively. This material is available free of charge via the Internet at <http://pubs.acs.org>.

References and Notes

- (1) Heine, A.; Herbst-Irmer, R.; Stalke, D.; Kühnle, W.; Zachariasse, K. A. *Acta Crystallogr. B* **1994**, *50*, 363.
- (2) Sinclair, W. E.; Pratt, D. W. *J. Chem. Phys.* **1996**, *105*, 7942.
- (3) Kerstel, E. R. Th.; Becucci, M.; Pietraperzia, G.; Castellucci, E. *Chem. Phys.* **1995**, *199*, 263.
- (4) Lister, D. G.; Tyler, J. K.; Hog, J. H.; Larson, N. W. *J. Mol. Struct.* **1974**, *23*, 253.
- (5) Tzeng, W. B.; Narayanan, K.; Shieh, K. C.; Tung, C. C. *J. Mol. Struct.* **1998**, *428*, 231.
- (6) Schultz, G.; Portalone, G.; Ramondo, F.; Domenicano, A.; Hargittai, I. *Struct. Chem.* **1996**, *7*, 59.
- (7) Tzeng, W. B.; Narayanan, K. *J. Mol. Struct.* **1998**, *446*, 93.
- (8) Powers, D. E.; Hopkins, J. B.; Smalley, R. E. *J. Chem. Phys.* **1980**, *72*, 5721.
- (9) Wategaonkar, S.; Doraiswamy, S. *J. Chem. Phys.* **1997**, *106*, 4894.
- (10) Wategaonkar, S.; Doraiswamy, S. *J. Chem. Phys.* **1996**, *105*, 1786.
- (11) Tzeng, W. B.; Narayanan, K.; Hsieh, C. Y.; Tung, C. C. *J. Chem. Soc., Faraday Trans.* **1997**, *93*, 2981.

- (12) Sugawara, K.; Miyawaki, J.; Nakanaga, T.; Takeo, H.; Lembach, G.; Djafari, S.; Barth, H.-D.; Brutschy, B. *J. Phys. Chem.* **1996**, *100*, 17145.
- (13) Fukuyo, M.; Hirotsu, K.; Higuchi, T. *Acta Crystallogr. B* **1982**, *38*, 640.
- (14) Trueblood, K. N. *Acta Crystallogr.* **1961**, *14*, 1009.
- (15) Collings, P. J.; Hird, M. *Introduction to Liquid Crystals Chemistry and Physics*; Taylor and Francis: London, 1997.
- (16) Felker, P. M. *J. Phys. Chem.* **1992**, *96*, 7844.
- (17) Riehn, C.; Weichert, A.; Zimmermann, M.; Brutschy, B. *Chem. Phys. Lett.* **1999**, *299*, 103.
- (18) Riehn, C.; Weichert, A.; Lommatzsch, U.; Zimmermann, M.; Brutschy, B. *J. Chem. Phys.* **2000**, *112*, 3650.
- (19) Sheldrick, G. M. SADABS, Program for Empirical Absorption Correction of Area Detector Data, University of Göttingen, Germany, 1996.
- (20) Sheldrick, G. M. SHELXS-97, Program for the Solution of Crystal Structures, University of Göttingen, Germany, 1997.
- (21) Sheldrick, G. M. SHELXL-97, Program for the Structure Refinement, University of Göttingen, Germany, 1997.
- (22) Sheldrick, G. M. SHELXTL-Plus, Release 5.03, Siemens Analytical X-ray Instruments Inc., Madison, WI, 1997.
- (23) Baskin, J. S.; Felker, P. M.; Zewail, A. H. *J. Chem. Phys.* **1986**, *84*, 4708.
- (24) Hollas, J. M. *High-Resolution Spectroscopy*, 2nd ed.; J. Wiley & Sons: Chichester, UK, 1998.
- (25) Côté, M. J.; Kauffman, J. F.; Smith, P. G.; McDonald, J. D. *J. Chem. Phys.* **1989**, *90*, 2865.
- (26) Kauffman, J. F.; Côté, M. J.; Smith, P. G.; McDonald, J. D. *J. Chem. Phys.* **1989**, *90*, 2874.
- (27) Felker, P. M.; Zewail, A. H. In *Femtochemistry*; Manz, J., Wöste, L., Ed.; VCH: Weinheim, Germany, 1995, Chapter 5, Vol. I.
- (28) *Gaussian 94*, Revision D.4; Frisch, M. J.; Trucks, G. W.; Schlegel, H. B.; Gill, P. M. W.; Johnson, B. G.; Robb, M. A.; Cheeseman, J. R.; Keith, T.; Petersson, G. A.; Montgomery, J. A.; Raghavachari, K.; Al-Laham, M. A.; Zakrzewski, V. G.; Ortiz, J. V.; Foresman, J. B.; Cioslowski, J.; Stefanov, B. B.; Nanayakkara, A.; Challacombe, M.; Peng, C. Y.; Ayala, P. Y.; Chen, W.; Wong, M. W.; Andres, J. L.; Replogle, E. S.; Gomperts, R.; Martin, R. L.; Fox, D. J.; Binkley, J. S.; Defrees, D. J.; Baker, J.; Stewart, J. J. P.; Head-Gordon, M.; Gonzalez, C.; Pople, J. A. Gaussian, Inc.: Pittsburgh, PA, 1995.
- (29) Lampert, H.; Mikenda, W.; Karpfen, A. *J. Phys. Chem. A* **1997**, *101*, 2254.
- (30) Unpublished results.
- (31) Berden, G.; van Rooy, J.; Meerts, W. L.; Zachariasse, K. A. *Chem. Phys. Lett.* **1997**, *278*, 373.
- (32) Lommatzsch, U.; Brutschy, B. *Chem. Phys.* **1998**, *234*, 35.
- (33) The wagging angle has been determined as the angle between the plane of the amino group ($\angle\text{H}(1\text{A})-\text{N}-\text{H}(1\text{B})$) and the least-squares plane of the carbon atoms of the aromatic ring (C(1) through C(6)). There is a small difference to the data of ref 18, due to the fact that the wagging angle was determined between the amino group and the plane of the carbon atoms C(1), C(2), and C(3) of the aromatic ring and a different level for the ab initio calculation (HF/6-31G(d)).
- (34) Smith, P. G.; Troxler, T.; Topp, M. R. *J. Phys. Chem.* **1993**, *97*, 6983.
- (35) Čížský, P. *Encyclopedia of Computational Chemistry*; Schleyer, P. v. R., Ed.; John Wiley & Sons Inc.: New York, 1998.
- (36) Orlandi, G.; Palmieri, P.; Tarroni, R.; Zerbetto, F.; Zgierksi, M. Z. *J. Chem. Phys.* **1994**, *100*, 2458.
- (37) Zilberg, S.; Haas, Y. *J. Chem. Phys.* **1995**, *103*, 20.
- (38) In ref 18 two slightly different sets (I and II) of rotational constants have been obtained to fit the experimental data. Due to overlapping transient recurrences no unambiguous assignment was obtained. But with additional information set (II) was found favorable for the description of the excited state. This assignment was confirmed recently by a high-resolution stimulated emission pumping (SEP) RCS experiment in our group.